AFRL-AFOSR-VA-TR-2016-0194

Multi-Chromatic Ultrashort Pulse Filamentation and Bulk Modification in Dielectrics

Jeremy Gulley
KENNESAW STATE UNIVERSITY

05/05/2016
Final Report

Air Force Research Laboratory
AF Office Of Scientific Research (AFOSR)/ RTB1
Arlington, Virginia 22203
Air Force Materiel Command

REPORT DOCUMENTATION PAGE

Form Approved
OMB No. 0704-0188

PLEASE DO NOT RETURN YOUR FORM TO THE ABOVE ORGANIZATION.

1. REPORT DATE *(DD-MM-YYYY)*	2. REPORT TYPE	3. DATES COVERED *(From - To)*
29-04-2016	Final Report	01 Feb 2013 - 31 Jan 2016

4. TITLE AND SUBTITLE

Multi-chromatic Ultrashort Pulse Filamentation and Bulk Modification in Dielectrics

5a. CONTRACT NUMBER

5b. GRANT NUMBER

FA9550-13-1-0069

5c. PROGRAM ELEMENT NUMBER

6. AUTHOR(S)

Dr. Jeremy Gulley

5d. PROJECT NUMBER

5e. TASK NUMBER

5f. WORK UNIT NUMBER

7. PERFORMING ORGANIZATION NAME(S) AND ADDRESS(ES)

Kennesaw State University
Department of Physics
370 Paulding Rd., MD 1204

8. PERFORMING ORGANIZATION REPORT NUMBER

9. SPONSORING/MONITORING AGENCY NAME(S) AND ADDRESS(ES)

Air Force Office of Scientific Research
875 North Randolph Road
Arlington, VA 22203

10. SPONSOR/MONITOR'S ACRONYM(S)

AFOSR

11. SPONSOR/MONITOR'S REPORT NUMBER(S)

12. DISTRIBUTION/AVAILABILITY STATEMENT

Approved for public release; distribution is unlimited.

13. SUPPLEMENTARY NOTES

AFOSR Program Manager: Dr. Arje Nachman

14. ABSTRACT

This research investigated filamentation in, and modification of, dielectric solids by multi-chromatic ultrashort laser pulses. It was a theoretical effort to develop models of multi-chromatic laser-material interactions in bulk solids and couple these to pulse propagation simulations. The research developed techniques to control filamentation and the onset of laser-induced bulk damage with multi-chromatic pulses. This included controlling modification and filamentation in solids using co-propagating laser pulses of different frequencies as well as strongly chirped pulses and spatially chirped annular pulses. Emphasis was placed on nonlinear optical propagation effects since they determine the field distribution at the laser focus, the control of which is necessary for progress in laser bulk micro-machining towards nano-machining. Computationally efficient 3D quantum models of laser-induced photoionization and the electronic Kerr effect were developed for coupling with the already established pulse propagation methods.

15. SUBJECT TERMS

Nonlinear optics, ultrashort laser pulses, propagation, femtosecond laser filamentation, laser-induced modification

16. SECURITY CLASSIFICATION OF:			17. LIMITATION OF ABSTRACT	18. NUMBER OF PAGES	19a. NAME OF RESPONSIBLE PERSON
a. REPORT	b. ABSTRACT	c. THIS PAGE			Dr. Jeremy Gulley
Unclassified	Unclassified	Unclassified	Unlimited	21	19b. TELEPHONE NUMBER *(Include area code)* 470-578-2933

Reset

Standard Form 298 (Rev. 8/98)
Prescribed by ANSI Std. Z39.18
Adobe Professional 7.0

REPORT DOCUMENTATION PAGE

Form Approved
OMB No. 0704-0188

PLEASE DO NOT RETURN YOUR FORM TO THE ABOVE ORGANIZATION.

1. REPORT DATE *(DD-MM-YYYY)*	2. REPORT TYPE	3. DATES COVERED *(From - To)*
29-04-2016	Final Report	01 Feb 2013 - 31 Jan 2016

4. TITLE AND SUBTITLE

(YIP) Multi-chromatic Ultrashort Pulse Filamentation and Bulk Modification in Dielectrics

5a. CONTRACT NUMBER

5b. GRANT NUMBER

FA9550-13-1-0069

5c. PROGRAM ELEMENT NUMBER

6. AUTHOR(S)

Jeremy R. Gulley

5d. PROJECT NUMBER

5e. TASK NUMBER

5f. WORK UNIT NUMBER

7. PERFORMING ORGANIZATION NAME(S) AND ADDRESS(ES)

Kennesaw State University
Department of Physics
370 Paulding Rd., MD 1204

8. PERFORMING ORGANIZATION REPORT NUMBER

9. SPONSORING/MONITORING AGENCY NAME(S) AND ADDRESS(ES)

Air Force Office of Scientific Research
875 North Randolph Road
Arlington, VA 22203

10. SPONSOR/MONITOR'S ACRONYM(S)

AFOSR

11. SPONSOR/MONITOR'S REPORT NUMBER(S)

12. DISTRIBUTION/AVAILABILITY STATEMENT

Approved for public release; distribution is unlimited.

13. SUPPLEMENTARY NOTES

AFOSR Program Manager: Dr. Arje Nachman

14. ABSTRACT

This research investigated filamentation in, and modification of, dielectric solids by multi-chromatic ultrashort laser pulses. It was a theoretical effort to develop models of multi-chromatic laser-material interactions in bulk solids and couple these to pulse propagation simulations. The research developed techniques to control filamentation and the onset of laser-induced bulk damage with multi-chromatic pulses. This included controlling modification and filamentation in solids using co-propagating laser pulses of different frequencies as well as strongly chirped pulses and spatially chirped annular pulses. Emphasis was placed on nonlinear optical propagation effects since they determine the field distribution at the laser focus, the control of which is necessary for progress in laser bulk micro-machining towards nano-machining. Computationally efficient 3D quantum models of laser-induced photoionization and the electronic Kerr effect were developed for coupling with the already established pulse propagation methods.

15. SUBJECT TERMS

Nonlinear optics, ultrashort laser pulses, propagation, femtosecond laser filamentation, laser-induced modification

16. SECURITY CLASSIFICATION OF:			17. LIMITATION OF ABSTRACT	18. NUMBER OF PAGES	19a. NAME OF RESPONSIBLE PERSON
a. REPORT	b. ABSTRACT	c. THIS PAGE			Jeremy R. Gulley
Unclassified	Unclassified	Unclassified	Unlimited	21	19b. TELEPHONE NUMBER *(Include area code)* 470-578-2933

Reset

Standard Form 298 (Rev. 8/98)
Prescribed by ANSI Std. Z39.18
Adobe Professional 7.0

Multi-Chromatic Ultrashort Pulse Filamentation and Bulk Modification in Dielectrics

Contract FA9550-13-1-0069
Final Report
February 2013 – January 2016

Submitted to: Air Force Office of Scientific Research
ATTN: Dr. Arje Nachman
875 North Randolph Road
Arlington, VA 22203

Submitted by: Kennesaw State University
Department of Physics
Kennesaw, GA 30144

Principal Investigator: Jeremy R. Gulley

April, 29 2016

Contents

ABSTRACT

This research investigated filamentation in, and modification of, dielectric solids by multi-chromatic ultrashort laser pulses. Filamentation of ultrashort laser pulses is a phenomenon with a growing pool of applications in communications and national defense. Ultrafast laser systems can also affect a wide variety of micrometer and nanometer scale modifications to dielectrics and semiconductors. This research was a theoretical effort to develop comprehensive models of multi-chromatic laser-material interactions in bulk solids and couple them to pulse propagation simulaisions. The research investigated techniques to control filamentation and the onset of laser-induced bulk modification with multi-chromatic pulses. This included controlling modification and filamentation in solids using co-propagating laser pulses of different frequencies as well as strongly chirped pulses and spatially chirped annular pulses. Emphasis was placed on nonlinear optical propagation effects since they determine the field distribution at the laser focus, the control of which is necessary for progress in laser bulk micro-machining towards nano-machining. Propagation simulations were coupled to newly developed extended multi-rate equation methods to model the free-carrier distribution evolution in the energy space when exposed to strongly chirped pulses. Computationally efficient 3D quantum models of laser-solid interactions were also developed for coupling with the extended multi-rate equations and already established pulse propagation methods. Coupling this model to 3D pulse propagation and comparing the results to a collaborative experiment conducted at AFRL are in progress at the time of this report. This work was sponsored by the Air Force Office of Scientific Research (AFOSR) within the Young Investigator Program.

1 Summary

1.1 Overview

This funding fully supported a postdoc for all but four months of the grant's duration, as well as the PI's summer salary for 4.5 months. In addition to travel and publication funds, the grant also paid for one travel laptop, one visualization desktop unit, and two computational servers. The research supported by this grant is disseminated in eight publications, one paper currently under review, two papers in preparation, and six conference presentations. Each of these works, with the exception of the collaborative paper under review, were fully supported by this funding and are summarized below.

1.2 Publications

- J. R. Gulley, J. Liao, and T. E. Lanier, "Plasma generation by ultrashort multi-chromatic pulses during nonlinear propagation," *Frontiers in Ultrafast Optics: Biomedical, Scientific, and Industrial Application XIV*, Proc. SPIE Int. Soc. Opt. Eng. **8972**, 89720T (2014).

- J. Liao and J. R. Gulley, "Time-frequency control of ultrafast plasma generation in dielectrics," *J. Opt. Soc. Am. B* **31**, 2973-2980 (2014).
- J. R. Gulley and T. E. Lanier,"Model for ultrashort laser-pulse induced ionization dynamics in transparent solids," *Phys. Rev. B.* **90**, 155119 (2014).
- T. E. Lanier and J. R. Gulley, "Annular space-time focusing in fused silica," *Frontiers in Optics 2015*, OSA Technical Digest, paper FTu5E.6 (2015).
- J. R. Gulley and T. E. Lanier, "Self-consistent modeling of photoionization and the Kerr effect in bulk solids," *Laser-Induced Damage in Optical Materials: 2015*, Proc. SPIE Int. Soc. Opt. Eng. **7632**, 96320X (2015).
- T. E. Lanier and J. R. Gulley, "Calculation of nonlinear optical damage from space-time-tailored pulses in dielectrics," *Laser-Induced Damage in Optical Materials: 2015*, Proc. SPIE Int. Soc. Opt. Eng. **9632**, 96320Z (2015).
- T. E. Lanier and J. R. Gulley, "Nonlinear space-time focusing and filamentation of annular femtosecond pulses in dielectrics," *J. Opt. Soc. Am. B* **33**, 292-301 (2016).
- K. Huthmacher, A. K. Molberg, B. Rethfeld, and J. R. Gulley, "A C++11/Fortran 2003 interface to include electron-electron collisions via Monte Carlo in Multiple Rate Equation simulations," *J. Comput. Phys.* (under review).
- J. R. Gulley and T. E. Lanier, "Self-consistent modeling of photoionization and nonlinear optics in cubic dielectric solids," (in preparation).
- T. E. Lanier and J. R. Gulley, "Two pulse multi-frequency induced modification in optical glasses," (in preparation).

1.3 Presentations

- J. R. Gulley, J. Liao, and T. E. Lanier,"Plasma generation by ultrashort multi-chromatic pulses during nonlinear propagation," Proc. SPIE 8972, Frontiers in Ultrafast Optics: Biomedical, Scientific, and Industrial Application XIV, San Francisco, CA (2014).
- J. R. Gulley, "Self-consistent modeling of photoionization for nonlinear pulse propagation in solids," Progress in Electromagnetics Research Symposium, Prague, Czech Republic (2015).
- T. E. Lanier and J. R. Gulley, "Calculation of nonlinear optical damage from space-time-tailored pulses in dielectrics," Laser-Induced Damage in Optical Materials: 2015, Boulder, CO (2015).
- J. R. Gulley and T. E. Lanier, "Self-consistent modeling of photoionization and the Kerr effect in bulk solids," Laser-Induced Damage in Optical Materials: 2015, Boulder, CO (2015).

- T. E. Lanier and J. R. Gulley, "Annular space-time focusing in fused silica," Frontiers in Optics 2015, San Jose, CA (2015).
- J. R. Gulley, "Self-consistent modeling of photoionization and nonlinear optics in dielectrics," High Power Laser Ablation / Directed Energy Symposium, Santa Fe, NM (2016).

2 Introduction

The goal of this project was to model nonlinear ultrashort laser pulse propagation and to develop techniques that make novel use of their unique multi-chromatic properties. Traditionally, propagation simulations studying ultrashort pulse filamentation and bulk modification include an internal contradiction for the case of solids: they combine time-dependent pulse amplitudes with the monochromatic approximation underlying the electron-plasma and ionization models. Absence of an adequate model that accounts for the multi-chromatic nature of ultrashort laser pulses has precluded progress in the applications of pulse filamentation, as well as important techniques of micromachining and nanofabrication in transparent solids. This project set out to couple comprehensive models of photoionization and multiphoton absorption by ultrashort laser pulses with a newly developed, comprehensive model of laser interactions with the generated conduction electrons. These models were then integrated into the modeling of pulse propagation. Additionally, two cases of interest were investigated for controlling filamentation and bulk modifications that utilize the multi-chromatic nature of the fields (multi-frequency multi-pulse fields and chirped pulses). The specific objectives of the project were:

1) Develop a multi-chromatic model of solid-state plasma dynamics that generates a free-current density for use in Maxwell's equations.

2) Integrate this model into a numerical code to simulate ultrashort-pulse propagation and filamentation in dielectric solids.

3) Simulate high-power ultrafast propagation and bulk modification by multi-chromatic laser pulses in solids for two specific applications:
(a) strongly chirped pulses.
(b) two co-propagating pulses of different frequencies.

4) Develop non-time-averaged multi-chromatic quantum-mechanical models of photoionization and the Kerr effect in dielectric solids by ultrashort laser pulses.

The remainder of this report summarizes the accomplishments and progress towards these ends. Where the details of research findings are available in published form, the papers are cited in the section titles and the most important results are discussed. Where the research is not yet published, more detailed descriptions are provided.

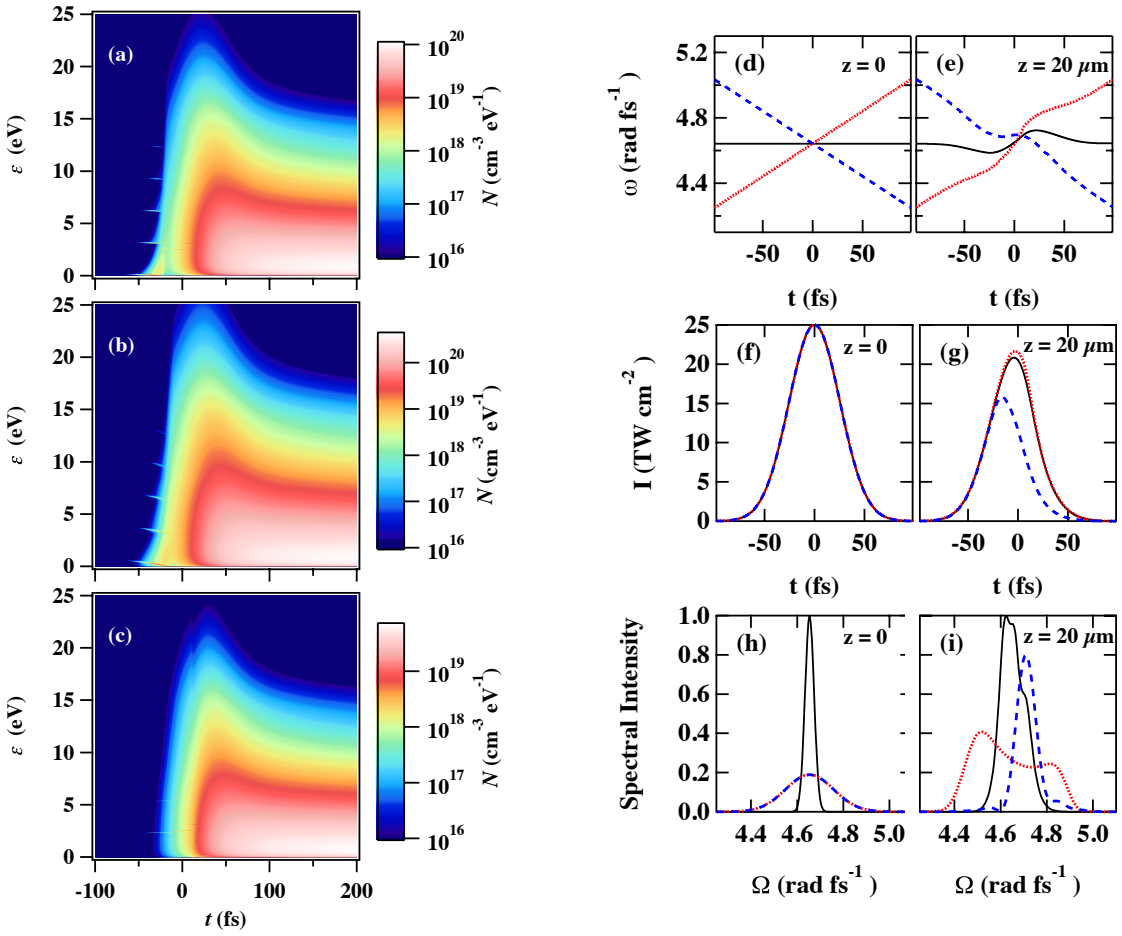

Figure 1: On the left side: electron energy distributions after exposure to (a) an unchirped pulse, (b) a negatively chirped pulse, and (c) a positively chirped pulse. On the right side: the instantaneous frequency (d) and (e), intensity (f) and (g), and normalized transmitted spectra (h) and (i), at propagation distances of z = 0 and 20 m, respectively. The negatively chirped pulse is shown as the blue dashed line, the unchirped pulse is shown as the black solid line, and the positively pulse is shown as the red dotted line.

3 Modeling of ionization and propagation in dielectrics by strongly chirped pulses [1-2]

A comprehensive model of ultrafast laser-induced plasma dynamics intended for coupling with pulse propagation simulations in transparent solids was developed. The model comprised two sets of extended multi-rate equations for the free-carrier distribution and the free-current density. The changing spectrum of a propagating ultrashort laser pulse was taken into account by use of the instantaneous frequency in calculating photoionization and single-photon absorption rates. It simultaneously coupled to the evolution of the energy-resolved nonequilibrium free-carrier distribution, which was examined as a function of time (see left side of Fig. 1). The model accounted for the distribution dependence of electron-phonon and electron-electron collision times in the distribution evolution as well as free-carrier absorption, each using relaxation approximations.

Our simulations solved this model in fused silica for strongly chirped pulses (shown Fig. 1). The results suggest that strong pulse chirps, such as those occurring naturally during nonlinear propagation, lead to ionization dynamics that are not captured by the standard monochromatic treatment of laser-induced plasma formation. The order-of-magnitude chirp-dependent differences in ionization yield and the electron distribution shapes govern the strength and character of the laser-plasma interactions. The proposed model therefore provides a framework for laser-material interactions that is practical and provides better insight into the physics of laser-induced ionization by intense ultrashort laser pulses. Propagation of these pulses over 20 μm demonstrates how the multi-chromatic nature of oppositely chirped pulses alters the pulse and spectral evolution due to ionization. Fully 3D pulse propagation simulations using this extended multi-rate equation approach also demonstrates a chirp dependence on the shape and localization of ionization regions in the material. The use of the instantaneous frequency (which is not always meaningful) should only be used when a central frequency can still be well defined. The intent of this model is to unify it with the optical Bloch equation methods described later in Sec. 7, thus providing a simultaneous quantum mechanical treatment of ionization and Kerr effect while treating the many-body effects using the relaxation approximation.

4 Ultrafast ionization in dielectrics with stochastic modeling of electron-electron collisions [3]

In addition to the extended multi-rate equation described in Sec. 3, we developed a split-step numerical method for calculating ultrafast free-electron dynamics in a collaboration with the group of Dr. Baerbel Rethfeld at the University of Kaiserslautern in Germany. The first step of the split-step approach solves a the ordinary deterministic extended multi-rate equation for the ionization, electron-phonon collisions, and single photon absorption by free-carriers. The second step is stochastic and models electron-electron collisions by solving the Boltzmann scattering equation using Monte-Carlo techniques, thus eliminating the need for a relaxation treatment of electron-electron collisions which are the dominant force in reshaping the non-equilibrium distribution. This combination of deterministic and

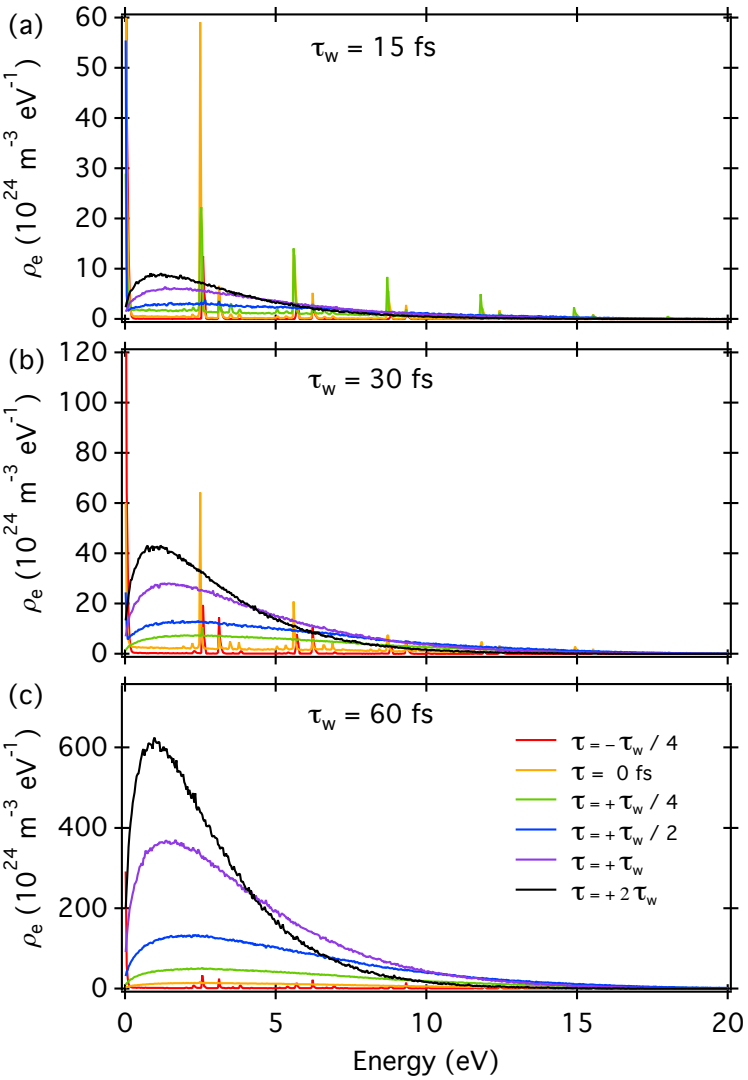

Figure 2: Conduction band electron distributions in fused silica as functions of electron energy at various times for 400 nm pulses with peak intensities of 4×10^{13} W/cm^2 and durations of (a) $\tau_{\rm w} = 15$ fs, (b) $\tau_{\rm w} = 30$ fs, and (c) $\tau_{\rm w} = 60$ fs.

stochastic approaches is a unique and efficient method of calculating the nonlinear dynamics of 3D materials exposed to high intensity ultrashort pulses. The results in Fig. 2 from simulations solving the split-step model in fused silica demonstrate that electron-electron scattering relaxes the non-equilibrium electron distribution on the order of 15 fs, during the exposure to ultrashort pulses. We also coupled this model with pulse propagation, and where identical pulses and material parameters are assumed the results agree very well with those of the extended multi-rate equation using the relaxation approximation, which is much faster. A continued collaboration to also treat the important impact ionization stochastically is on-going.

5 Simple modeling of bulk modification by multi-frequency, multi-pulse fields [4]

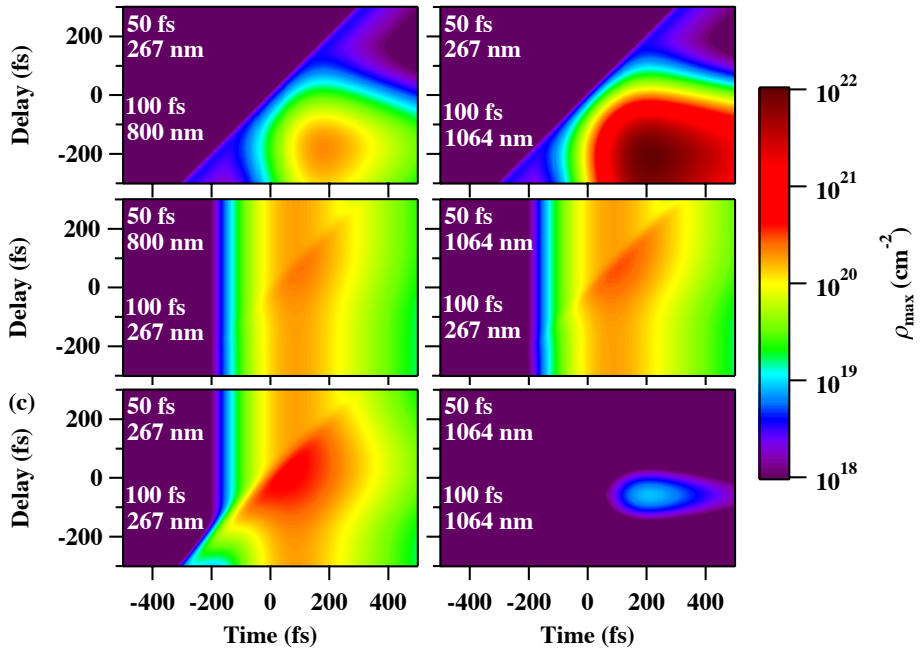

Figure 3: Ionization yields generated in fused silica by 50 fs - 250 fs double-pulse trains as functions of time (given in the reference frame of the 250 fs pulse) and delay between the two pulses. The 50 fs and 250 fs pulses have wavelengths as labeled and respective peak intensities of 1×10^{12} W/cm^2 and 4×10^{12} W/cm^2.

In the recent ultrashort laser-induced micromachining literature there has been increased interest in experiments using multi-color, two-pulse fields. Typically, this involves using a high frequency, low energy pulse to drive photoionization followed by a low frequency, high energy pulse to drive avalanching. To date, the experimental papers using this technique attempt to verify this approach by modeling the ionization with oversimplified 1D propagation models combined with one or two rate equations to calculate the ionization. To

facilitate a fast and effective modeling for time-frequency control of plasma generation for fully 3D propagation simulations, we developed a modified ordinary multi-rate equation to calculate ionization by double-pulses of different frequencies. This model also discretizes the conduction electron distribution in energy space, but with levels equal to the smallest photon energy of the low-frequency pulse. The approach is comparable in computational speed to the ubiquitous single rate equation for ionization in the filamentation literature. We used this approach to calculate the optimal experimental delay between pulses of particular frequencies, energies and pulsewidths (see Fig. 3). In practice, the first of these pulses is usually a harmonic of the second pulse at the fundamental frequency. However, the Fig. 3 results on the right side show that non-harmonic double-pulse trains can control plasma generation with a minimal fluence while still using common laser frequencies.

6 Control of filamentation and bulk modification by spatio-temporally chirped pulses [5-7]

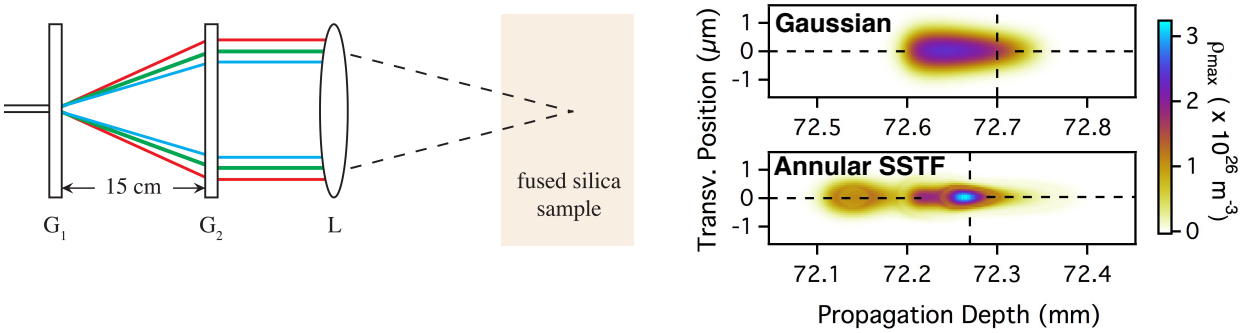

Figure 4: On the left: a schematic of the simulated SSTF system comprising two concentric gratings G_1 and G_2 with ring spacing $d = 10$ μm and a lens of focal length $f = 200$ mm. On the right: ionization tracks for 0.5-μJ (a) Gaussian beam-pulse with initial an pulsewidth of 40 fs and (b) SSTF annular pulse of approximately 40 fs pulsewidth at the linear focus.

Filamentation during simultaneous space-time focusing in bulk fused silica was investigated numerically for spatially chirped annular pulses. We modeled the use of a pair of concentric gratings to transform a common femtosecond laser pulse with Gaussian spatial profile into a radially chirped, annular beam shape that is focused into the bulk of silica by a lens. The system schematic for this setup is shown on the left side of Fig. [4]. Pulse propagation simulations compared the ionization yields of these annular space-time focusing waveforms as functions of beam radius and propagation distance, and are compared to those of ordinary gaussian pulses of the same numerical aperture, shown on the right side of Fig. [4]. The results show that slightly higher ionization yields, and greater radial localization of the peak structure of these yields on the micro-nanometer scale, are possible with the annular space-time focusing configuration. This is significant since the regions of peak ionization yield often correlate with regions of laser-induced material modification in multi-shot experiments.

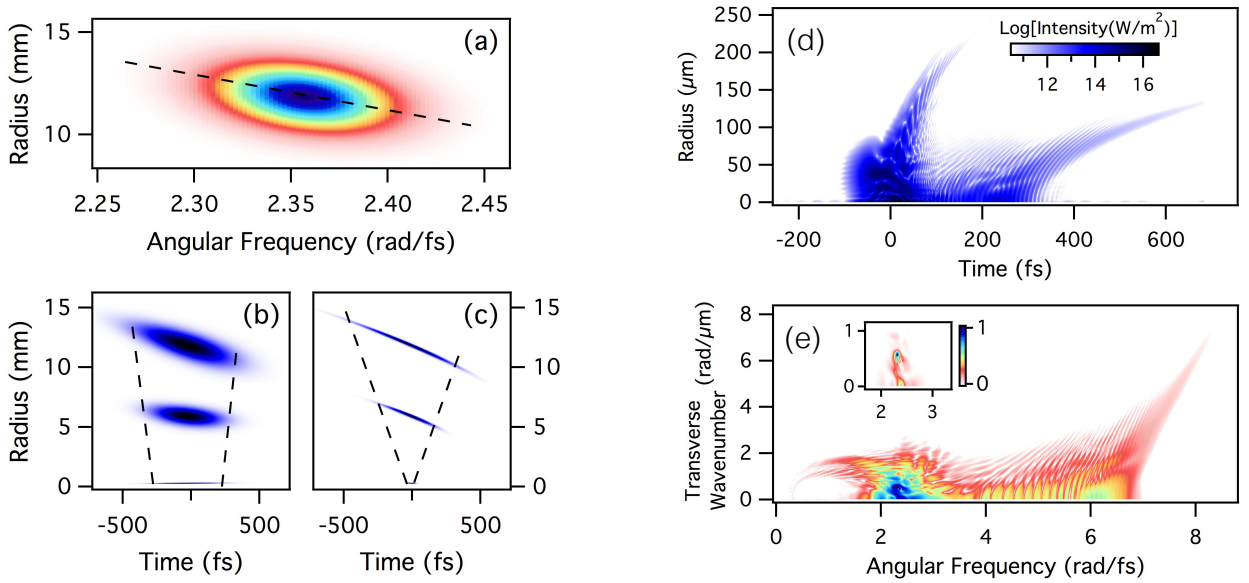

Figure 5: Left side shows SSTF in vacuum of annular pulses arising from radial chirp. (a) Tilted $r\omega$-spectrum just after G_2. (b)-(c) Normalized intensities at various z-positions (superposed). In each case, propagation distances as measured from the $f = 200$ mm lens are 0 mm (top), 100 mm (middle), and 195 mm (bottom). (b) The initially bandwidth-limited 40 fs pulse. (c) The positively pre-chirped pulse. Dashed lines are a guide for the eye. Right side shows the annular SSFT pulse just beyond the nonlinear focus for a 0.7-μJ pulse with optimal SSTF pre-chirp. (d) The log of the intensity (W/m^2) in rt-space. (e) Normalized intensity (inset), and the log of the normalized intensity (6 decades) in $k_\perp\omega$-space.

It is typically assumed that in simultaneous space-time focusing (SSTF) configurations the nonlinear propagation effects are approximately negligible. Our results confirm this outside of the nonlinear focal region, but inside the nonlinear focus the filamentation dynamics during the SSTF propagation play a non-negligible role in the pulse and material evolution. To acquire the optimal SSTF condition of a simultaneous minimum in both beam and pulse widths, one must vary the energy and/or time-chirp of the incident pulse (see left side of Fig. [5]). As the annular pulse propagates in the bulk silica we capture the field dynamics and material response that yields material modification and damage in the nonlinear focus. The propagation results show rich nonlinear dynamics typical of filamenting pulses, see right side of Fig. [5]. Thus, while higher ionization yields and greater spatial localization along the beam radius of these yields were obtained with annular SSTF pulses, such pulses were not effective at restricting the filamentation dynamics to the same length scales along the propagation axis.

7 Quantum modeling of photoionization and nonlinear optics in cubic solids [8]

In this section we describe results for modeling the laser-induced electron dynamics for a simple cubic 3D solid using a reduced set of Optical Bloch equations. It was important to move beyond the two-band approach originally proposed in the grant in order to calculate the Kerr effect and photoionization self-consistently. This approach calculates the contributions of photoionization, the Kerr effect, and current from free carriers in a self-consistent way that makes no assumptions about the pulse spectrum. In the perturbative nonlinear optical regime, the resulting polarization from this approach accurately reproduces the linear and nonlinear optical properties of wide-band gap cubic solids with corresponding multi-photon ionization. At higher field strengths corresponding to the non-perturbative nonlinear optical (tunneling) regime the polarization includes high-order harmonic generation due both to high order Kerr effects and Bragg reflection in the crystal. This approach calculates all orders of nonlinear optical polarizations resulting from electronic transitions from valance to conduction bands. The case of photoionization by multiple laser frequencies was examined in particular. Also, photoionization and the electronic Kerr effect are shown to be strongly coupled for ultrashort pulses on the order of 20 fs or less, contrary to the predictions of more traditional approaches. This is on the same time scale as the electron-electron collisions discussed in Sec. 4, and the intent in developing this approach is to merge it with the extended multi-rate equation for a comprehensive model of ionization and nonlinear optics. These results are still in preparation for publishing at the time of this report, so we provide theoretical detail sufficient to reproduce the presented results.

7.1 Multi-Band Laser-Solid Dynamics

The optical transitions in a multi-band 3D quasi-momentum space $\mathbf{k}$ can be calculated by the Semiconductor Bloch Equations (SBEs). On the femtosecond time scale the optical effects of many-body Coulomb processes can be modeled by a phenomenological dephasing rate γ, effectively reducing the Semiconductor Bloch Equations to a set of Optical-Bloch Equations. The time evolution of the occupation numbers for electrons ($f_{e_n,\mathbf{k}}$) and holes ($f_{h_n,\mathbf{k}}$), and the corresponding microscopic polarizations were generalized for multiband systems in the supplementary material of [O. Schuber, *et al.*, *Nat. Photon.* **8**, 119 (2014)]:

$$\frac{\partial f_{h_n,\mathbf{k}}}{\partial t} = -\frac{2}{\hbar}\mathrm{Im}\left[\sum_{h_l \neq h_n} d_{h_l h_n,\mathbf{k}} P^*_{h_n h_l,\mathbf{k}} + \sum_{e_l} d_{e_l h_n,\mathbf{k}} P^*_{h_n e_l,\mathbf{k}}\right] + \frac{|e|\,E(t)}{\hbar}\nabla_{\mathbf{k}} f_{h_n,\mathbf{k}}$$

$$\frac{\partial f_{e_n,\mathbf{k}}}{\partial t} = -\frac{2}{\hbar}\mathrm{Im}\left[\sum_{e_l \neq e_n} d_{e_n e_l,\mathbf{k}} P^*_{e_l e_n,\mathbf{k}} + \sum_{h_l} d_{e_n h_l,\mathbf{k}} P^*_{h_l e_n,\mathbf{k}}\right] + \frac{|e|\,E(t)}{\hbar}\nabla_{\mathbf{k}} f_{e_n,\mathbf{k}}$$

$$
\begin{aligned}
i\hbar\frac{\partial P_{h_m e_n,\mathbf{k}}}{\partial t} =& \left(\epsilon_{e_n,\mathbf{k}} + \epsilon_{h_m,\mathbf{k}} - i\hbar\gamma\right) P_{h_m e_n,\mathbf{k}} \\
&- d_{e_n h_m,\mathbf{k}} E(t)\left(1 - f_{e_n,\mathbf{k}} - f_{h_m,\mathbf{k}}\right) + |e|\, E(t) i\nabla_{\mathbf{k}} P_{h_m e_n,\mathbf{k}} \\
&+ E(t)\sum_{e_l \neq e_n}\left[d_{e_l h_m,\mathbf{k}} P_{e_l e_n,\mathbf{k}} - d_{e_n e_l,\mathbf{k}} P_{h_m e_l,\mathbf{k}}\right] \\
&+ E(t)\sum_{h_l \neq h_m}\left[d_{h_l h_m,\mathbf{k}} P_{h_l e_n,\mathbf{k}} - d_{e_n h_l,\mathbf{k}} P_{h_m h_l,\mathbf{k}}\right],
\end{aligned}
$$

$$
\begin{aligned}
i\hbar\frac{\partial P_{e_m e_n,\mathbf{k}}}{\partial t} =& \left(\epsilon_{e_n,\mathbf{k}} - \epsilon_{e_m,\mathbf{k}} - i\hbar\gamma\right) P_{e_m e_n,\mathbf{k}} \\
&- d_{e_n e_m,\mathbf{k}} E(t)\left(f_{e_m,\mathbf{k}} - f_{e_n,\mathbf{k}}\right) + |e|\, E(t) i\nabla_{\mathbf{k}} P_{e_m e_n,\mathbf{k}} \\
&+ E(t)\sum_{e_l \neq e_n} d_{e_l e_m,\mathbf{k}} P_{e_l e_n,\mathbf{k}} - E(t)\sum_{e_l \neq e_m} d_{e_n e_l,\mathbf{k}} P_{e_m e_l,\mathbf{k}} \\
&+ E(t)\sum_{h_l}\left[d_{h_l e_m,\mathbf{k}} P_{h_l e_n,\mathbf{k}} - d_{e_n h_l,\mathbf{k}} P^*_{h_l e_m,\mathbf{k}}\right],
\end{aligned}
$$

$$
\begin{aligned}
i\hbar\frac{\partial P_{h_m h_n,\mathbf{k}}}{\partial t} =& \left(\epsilon_{h_n,\mathbf{k}} - \epsilon_{h_m,\mathbf{k}} - i\hbar\gamma\right) P_{h_m h_n,\mathbf{k}} \\
&- d_{h_n h_m,\mathbf{k}} E(t)\left(f_{h_n,\mathbf{k}} - f_{h_m,\mathbf{k}}\right) + |e|\, E(t) i\nabla_{\mathbf{k}} P_{h_m h_n,\mathbf{k}} \\
&+ E(t)\sum_{e_l}\left[d_{e_l h_m,\mathbf{k}} P^*_{h_n e_l,\mathbf{k}} - d_{h_n e_l,\mathbf{k}} P_{h_m e_l,\mathbf{k}}\right] \\
&+ E(t)\sum_{h_l \neq h_n} d_{h_l h_m,\mathbf{k}} P_{h_l h_n,\mathbf{k}} - E(t)\sum_{h_l \neq h_m} d_{h_n h_l,\mathbf{k}} P_{h_m h_l,\mathbf{k}}.
\end{aligned}
$$

Here, $\epsilon_{h_m,\mathbf{k}}$ and $\epsilon_{e_n,\mathbf{k}}$ are the energies of the holes and electrons in the m^{th} and n^{th} bands, respectively. The terms with dipole matrix elements $d_{x_i y_j,\mathbf{k}}$ cause the interband transitions while the terms with $i\nabla_{\mathbf{k}}$ excite intraband activity. The laser field $E(t)$ is assumed to be linearly polarized. This model allows the inclusion of an arbitrary number of electron and hole bands, but the band structure must still be specified.

7.2 Band Structure

Our model is developed for laser-material interactions in a simple cubic solid. For the sake of simplicity while still retaining desirable band structure properties (*i.e.* non-parabolic shape, periodicity in quasi-momentum space, *etc.*) we use analytic formalisms to approximate the full 3D energy dispersion relations to ensure these properties. One possible model is the energy relation for a simple cubic medium in the nearest neighbor tight binding limit:

$$
\varepsilon_{n,\mathbf{k}} = \varepsilon_{n,\Gamma} + \Delta_n \sum_{i=x,y,z}\left(1 - \cos(k_i d)\right), \tag{1}
$$

where $\varepsilon_{n,\Gamma}$ is the electron energy of the n^{th} band at the Gamma point. The coefficients $\Delta_n = \hbar^2/(m_n d^2)$, d is the lattice constant, and m_n is the diagonal component of the electron effective mass tensor at $\mathbf{k} = 0$ for the n^{th} band.

Equation 1 is an instructive dispersion relation that we used to model a hypothetical 9 eV band gap crystal. However, to simulate a more realistic solid we chose the simple cubic crystal CsI. The nearest neighbor tight binding relation in Eq. 1 can be fitted to well approximate the valence bands in CsI when compared to theoretical calculations. Eq. 1 also fits well with the CsI conductions bands between the Γ-point and the X-point, but not between the Γ-point and the M-points or R-points. A better fit (although still not perfect) for the conduction bands is provided by the relation:

$$\varepsilon_{n,\mathbf{k}} = \varepsilon_{n,\Gamma} + \Delta_n - \Delta_n \cos(k_x d)\cos(k_y d)\cos(k_z d), \tag{2}$$

which has been used to approximate the transition energies in Alkalide Halides in the literature before [V. E. Gruzdev, *Phys. Rev. B* **75**, 205106 (2007)]. We therefore use Eq. 2 to approximate the structure of the CsI bands. All energies at the Γ-points are taken from the band calculations of [Y. Onodera, *J. Phys. Soc. Jap.* **25**, 469 (1968)], and the values for Δ_n are approximated from the calculated band structures by $\Delta_n = (\varepsilon_{n,X} - \varepsilon_{n,\Gamma})/2$. From this value we extract the approximate effective mass at each Γ-point, m_n.

7.3 Selection of dipole-matrix elements

Solving the SBEs with the desired band structure requires dipole-matrix elements $d_{ij,\mathbf{k}}$, which can be appreciably affected by the chosen band structure. In our calculations we vary the dipole coupling constant with momentum according to the well know relation $d_{cv,\mathbf{k}} = d_{cv,0}(\varepsilon_{c,\Gamma} - \varepsilon_{v,\Gamma})/(\varepsilon_{c,\mathbf{k}} - \varepsilon_{v,\mathbf{k}})$, but this still requires selecting a value for $d_{cv,0}$. While accounting first for necessary selection rules, the remaining values of $d_{cv,0}$ are estimated by $k \cdot p$ theory and then scaled to return the linear susceptibility as given by the sum over k-states

$$\chi^{(1)}_{\omega} = \sum_{c,v} \int_{BZ} \frac{4\left|d_{cv,\mathbf{k}}\right|^2}{(2\pi)^3 \epsilon_0} \frac{\varepsilon_{cv,\mathbf{k}}}{(\varepsilon_{cv,\mathbf{k}} - \hbar\omega - i\gamma)(\varepsilon_{cv,\mathbf{k}} + \hbar\omega + i\gamma)} d^3k.$$

The remaining dipole matrix elements are likewise chosen to return a reasonable value for the third-order susceptibility for long wavelengths $\chi^{(3)} \sim 10^{-18}\text{cm}^2/\text{V}^2$.

7.4 Reduction to effective 2D Calculation

The SBEs for a 3D solid can be solved directly in the 3D quasi-momentum space of the crystal, but this is computationally impractical for long distance propagation simulations. If the crystal structure is centro-symmetric and the laser field is linearly polarized along one of the crystal axes (assumed to be the z-direction), this procedure leads to many identical calculations that provide no new information. This is because the intrinsic inversion symmetry ensures that $f_{\text{n}}(k_x, k_y, k_z) = f_{\text{n}}(-k_x, -k_y, k_z)$ and $P_{\text{ij}}(k_x, k_y, k_z) = P_{\text{ij}}(-k_x, -k_y, k_z)$. One may not assume this inversion symmetry in all three directions since the presence of the laser field breaks the inversion symmetry in the direction of the field.

If the uniqueness of each calculation in a k_x-k_y plane at a particular k_z is determined by its associated electron (hole) energy $\varepsilon(\vec{k})$, then one need only solve each unique SBE and have knowledge of the effective density of states for that solution. To accomplish this reduction we transformed the (k_x, k_y, k_z) coordinate system to an effective 2D (Q_{xy}, k_z) system. Here the dimensionless coordinate Q_{xy} is a dimensionless coordinate that ranges from $-1 \leq Q_{xy} \leq 1$. The energies for the two band structures are then given by

$$\varepsilon_{n,\mathbf{k}} = \varepsilon_{n,\Gamma} + 3\Delta_n - \Delta_n \cos(k_z d) + 2\Delta Q_{xy}, \tag{3}$$

$$\varepsilon_{n,\mathbf{k}} = \varepsilon_{n,\Gamma} + \Delta_n - \Delta_n \cos(k_z d) Q_{xy}, \tag{4}$$

In either case, the effective density of states under this new coordinate system is given by

$$g(Q_{xy}, k_z) = \frac{2}{\pi^3 d^2} K\left[\sqrt{1 - Q_{xy}^2}\right]$$

which includes electron spin degeneracy. The function $K[X]$ is the complete elliptical integral of the first kind. With this simplification the SBEs for the full 3D momentum space can be solved in real time on the order of minutes (attempts to make futher simplification to an effective 1D-array calculation are on-going and would reduce the calculation time to the order of 1 s). Under this new coordinate system, the total ionization yield N_e, free current density $\vec{J}_f$, and total material polarization $\vec{P}$ are calculated by:

$$\begin{aligned}
N_e &= \sum_n \int_{\mathrm{BZ}} f_{e_n}(Q_{x,y}, k_z) g(Q_{x,y}, k_z) dQ_{xy} dk_z, \\
\vec{J}_F &= \sum_n \int_{\mathrm{BZ}} f_n(Q_{xy}, k_z) g(Q_{x,y}, k_z) \vec{j}_n(Q_{x,y}, k_z) dQ_{xy} dk_z, \text{ and} \\
\vec{P} &= \sum_{n,n'} \int_{\mathrm{BZ}} \vec{d}_{n,n'}(Q_{x,y}, k_z) P_{n,n'}(Q_{x,y}, k_z) g(Q_{x,y}, k_z) dQ_{xy} dk_z,
\end{aligned}$$

where $\vec{j}_n(\vec{k}) = (|e|/\hbar)\vec{\nabla}_{\mathbf{k}} \varepsilon_n(\vec{k})$.

7.5 Results for a three-band 9-eV simple cubic dielectric

The SBEs were solved for a hypothetical 9-eV simple cubic solid in the nearest neighbor tight binding limit. The three bands comprised a flat p-type valance band, one s-type conduction band, and one higher f-type conduction band. Parameters were chosen such that the linear and nonlinear refractive indices were $n_0 \approx 1.5$ and $n_2 \approx 3 \times 10^{-16}$ W/cm^2, respectively. For exposure to an 800 nm, 20 fs pulse with a peak intensity of 10 TW/cm^2, Fig. 6 shows the final occupation numbers in the first conduction band as a function of Q_{xy} and k_z. Here one can see the evidence of multi-photon absorption in the various rungs of the final electron distribution. We note that there were also electrons in the second conduction band, albeit with occupation numbers an order of magnitude or less than those of the first conduction band. The corresponding nonlinear polarization is shown in Fig. 7. Also shown in Fig. 7 is

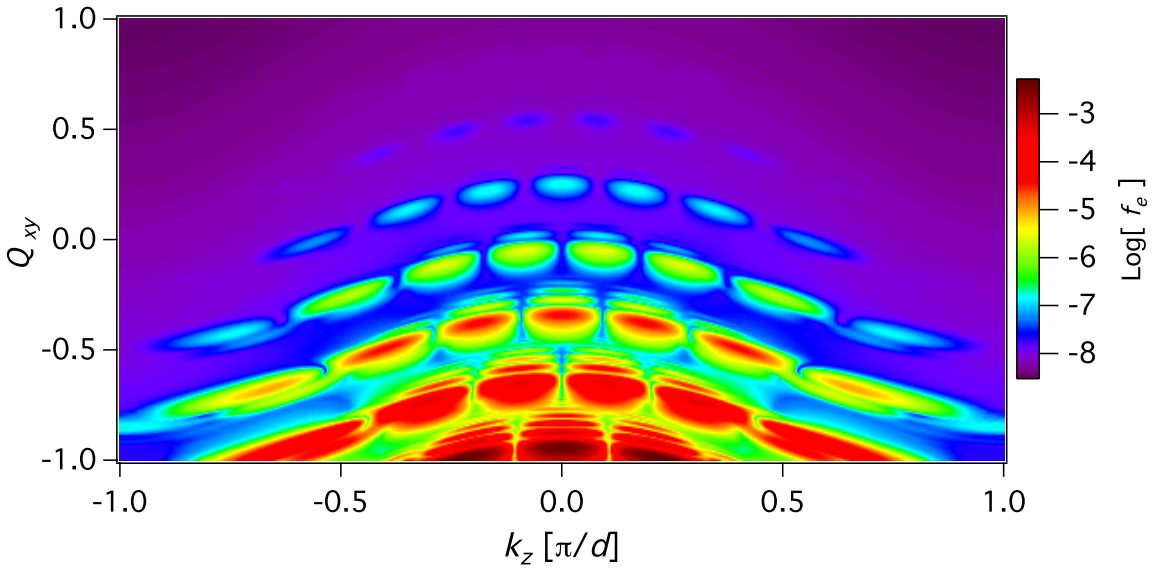

Figure 6: The occupation probability f_{e_1} as a function of the transverse coordinate Q_{xy} and the momentum k_z after exposure to a 20 fs, 800 nm laser pulse polarized in the z-direction.

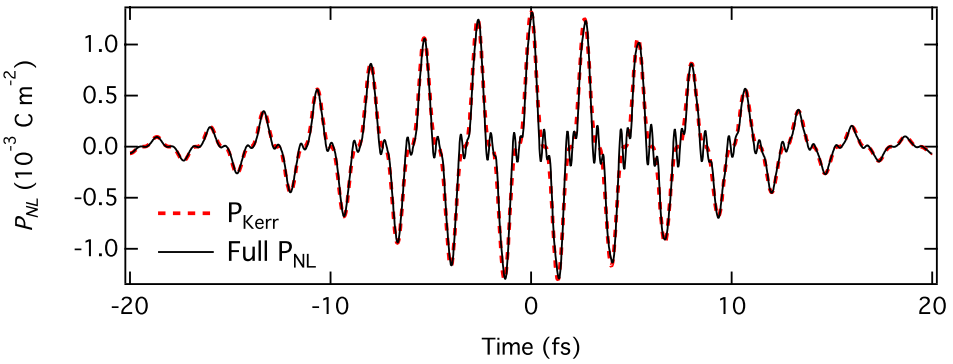

Figure 7: The calculated nonlinear polarization (solid-black line) and the traditional monochromatic Kerr-type polarization (dashed-red line) during exposure to a 20 fs, 800 nm laser pulse.

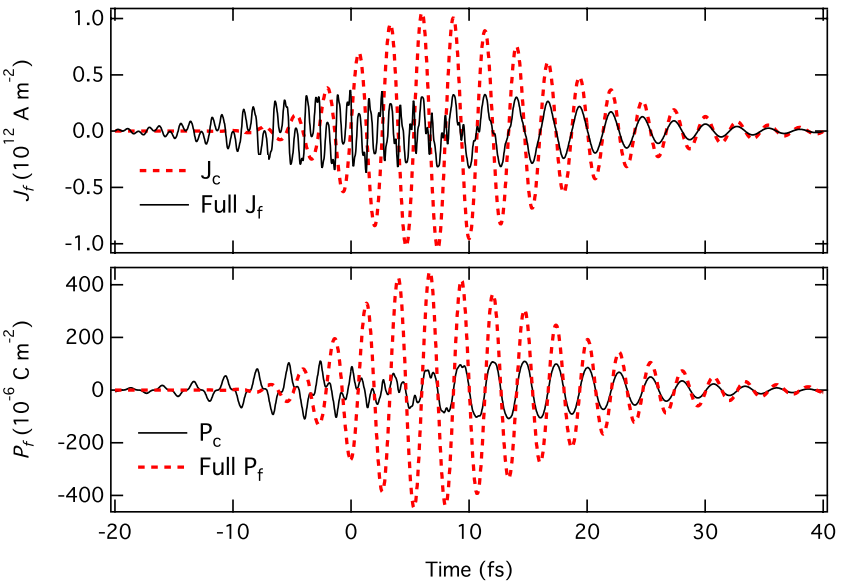

Figure 8: The calculated free current density (a) and free carrier polarization (b) as calculated by the SBEs (solid-black lines) and the classical free carrier current (dashed-red line) during exposure to a 20 fs, 800 nm laser pulse.

the calculation of the traditional Kerr effect $P_{\rm Kerr}(t) = \epsilon_0 \chi^{(3)} E^3(t)$. The agreement between the two models is initially good. As ionization increases, however, higher harmonics emerge in the full calculation.

Figure 8(a) shows the full current density calculation along with the classical free current density calculated by $J_c(t) = (e^2/m_r) \int_{-\infty}^{t} E(t) N_k(t) dt$, where $N_k(t)$ is the ionization yield calculated by the Keldysh model. Figure 8(b) show the time integrated values of both quantities in Figure 8(a) so that they appear as polarization contributions. Initially the full free polarization makes a contribution that is indistinguishable from the ordinary Kerr effect. Only after ionization occurs does the full free current match the form of the classical plasma current, which in turn leads to plasma defocusing of a laser beam, thus demonstrating that the separation of Kerr and ionization effects is artificial for intensities typical of filamentation and laser-induced damage in solids.

7.6 Results for seven-band CsI exposed to multi-harmonic fields

For a 7-band CsI simple cubic crystal we solved the SBEs for 20 fs pulses using Eq. 2 for the band structure. The three top valence bands, the three lowest conduction bands, and the lowest f-type conduction band were chosen to represent the band structure. For the 800 nm pulse in isolation, the post-exposure occupation numbers of the three lowest conduction bands are shown in Figure 9(a-c). The multi-photon ionization structure of these plots are difficult to interpret until one compares it to the conduction band energies as a function of the same coordinates, see Figure 9(d).

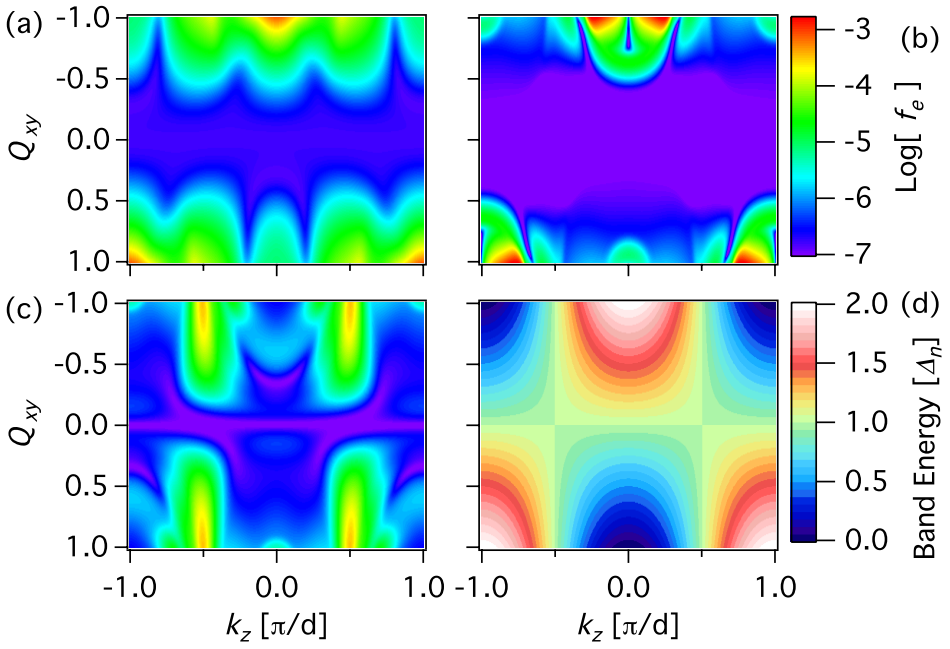

Figure 9: The occupation probabilities (a) f_{e_1}, (b) f_{e_2}, and (c) f_{e_3} as a function of the transverse energy Q_{xy} and the field-polarized momentum k_z after exposure to a 20 fs, 800 nm laser pulse. (d) The conduction band energy as a function of Q_{xy} and k_z.

We also solved the SBEs for other 20 fs single pulses and multi-color pulse combinations. One such case was for an 800 nm pulse of peak intensity 5 TW/cm^2, a 267 nm pulse of peak intensity 0.05 TW/cm^2, and both pulses present simultaneously. All the pulses are assumed to be Gaussian and centered about $t = 0$. Figure 10 shows the conduction electron populations as functions of time for each of these cases, the final population constituting the net yield. The 267 nm pulse in isolation had both the lowest intensity and the lowest yield, with the yield of the 800 nm pulse being an order of magnitude above it. However, the photoionization yield for the combined field increases by an order of magnitude, which is purely a multi-color photoionization effect which could be detectable in experiment. Nonlinear propagation simulations with such field combinations is challenging because the band gap of CsI (6.2 eV) straddles a two-photon absorption for the 267 nm pulse, and using a constant nonlinear refractive index is not valid for that field combination. Figure 10(c) shows the nonlinear polarization for the combined 800 nm and 267 nm field in the spectral domain. Here we note the presence of both even and odd order harmonics of the fundamental, which would not be predicted by a traditional Kerr effect calculation for this combind field. This is due primarily to the presence of multiple bands and would also not be captured by a two-band model.

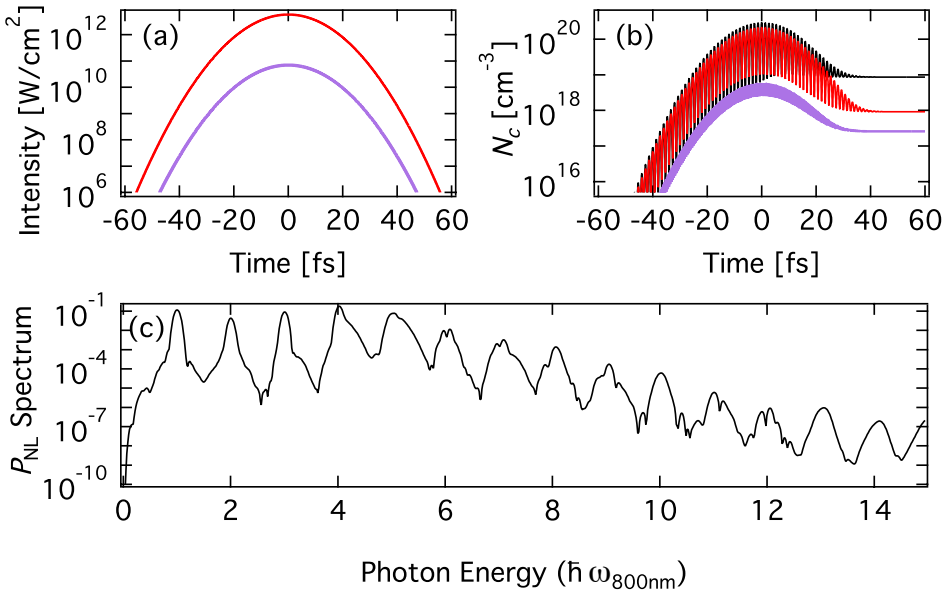

Figure 10: (a) The independent 800 nm (red) and 267 nm (purple) pulse intensities. (b) The total ionization yields for each individual pulse and for the combined fields (black). (c) The nonlinear polarization spectrum for the combined field in CsI.

8 Conclusions

This research investigated filamentation in, and modification of, dielectric solids by multi-chromatic ultrashort laser pulses through modeling and simulation. We simulated techniques to control filamentation and the onset of laser-induced bulk damage with multi-chromatic pulses using strongly chirped pulses and spatially chirped annular pulses. We developed extended multi-rate equation models for free-carrier dynamics of sufficient simplicity to couple with fully 3D pulse propagation simulations while accounting for many-body collisions using relaxation approximations and stochastic solving of a Boltamann scattering equation. We also developed a computationally efficient 3D quantum calculation of laser-solid coupling by solving a reduced set of Semiconductor Bloch Equations to obtain the source terms for propagation models and examined the solutions of this model for multi-chromatic pulse systems. This work is disseminated in eight papers (one under review), six conference presentations, and two papers in preparation at the time of this report.

9 Bibliography

1. J. R. Gulley, J. Liao, and T. E. Lanier, "Plasma generation by ultrashort multi-chromatic pulses during nonlinear propagation," *Frontiers in Ultrafast Optics: Biomedical, Scientific, and Industrial Application XIV*, Proc. SPIE Int. Soc. Opt. Eng. **8972**, 89720T (2014).

2. J. R. Gulley and T. E. Lanier,"Model for ultrashort laser-pulse induced ionization dynamics in transparent solids," *Phys. Rev. B.* **90**, 155119 (2014).

3. K. Huthmacher, A. K. Molberg, B. Rethfeld, and J. R. Gulley, "A C++11/Fortran 2003 interface to include electron-electron collisions via Monte Carlo in Multiple Rate Equation simulations," *J. Comput. Phys.* (under review).

4. J. Liao and J. R. Gulley, "Time-frequency control of ultrafast plasma generation in dielectrics," *J. Opt. Soc. Am. B* **31**, 2973-2980 (2014).

5. T. E. Lanier and J. R. Gulley, "Annular space-time focusing in fused silica," *Frontiers in Optics 2015*, OSA Technical Digest, paper FTu5E.6 (2015).

6. T. E. Lanier and J. R. Gulley, "Calculation of nonlinear optical damage from space-time-tailored pulses in dielectrics," *Laser-Induced Damage in Optical Materials: 2015*, Proc. SPIE Int. Soc. Opt. Eng. **9632**, 96320Z (2015).

7. T. E. Lanier and J. R. Gulley, "Nonlinear space-time focusing and filamentation of annular femtosecond pulses in dielectrics," *J. Opt. Soc. Am. B* **33**, 292-301 (2016).

8. J. R. Gulley and T. E. Lanier, "Self-consistent modeling of photoionization and the Kerr effect in bulk solids," *Laser-Induced Damage in Optical Materials: 2015*, Proc. SPIE Int. Soc. Opt. Eng. **7632**, 96320X (2015).

1.

1. Report Type

Final Report

Primary Contact E-mail

Contact email if there is a problem with the report.

jgulley@kennesaw.edu

Primary Contact Phone Number

Contact phone number if there is a problem with the report

470-578-2933

Organization / Institution name

Kennesaw State University

Grant/Contract Title

The full title of the funded effort.

(YIP) Multi-Chromatic Ultrashort Pulse Filamentation and Bulk Modification in Dielectrics

Grant/Contract Number

AFOSR assigned control number. It must begin with "FA9550" or "F49620" or "FA2386".

FA9550-13-1-0069

Principal Investigator Name

The full name of the principal investigator on the grant or contract.

Jeremy R. Gulley

Program Manager

The AFOSR Program Manager currently assigned to the award

Dr. Arje Nachman

Reporting Period Start Date

02/01/2013

Reporting Period End Date

01/31/2016

Abstract

This research investigated filamentation in, and modification of, dielectric solids by multi-chromatic ultrashort laser pulses. It was a theoretical effort to develop models of multi-chromatic laser-material interactions in bulk solids and couple these to pulse propagation simulations. The research developed techniques to control filamentation and the onset of laser-induced bulk damage with multi-chromatic fields. This included controlling modification and filamentation in solids using co-propagating laser pulses of different frequencies as well as strongly chirped pulses and spatially chirped annular pulses. Emphasis was placed on nonlinear optical propagation effects since they determine the field distribution at the laser focus, the control of which is necessary for progress in laser bulk micro-machining towards nano-machining. Computationally efficient 3D quantum models of laser-induced photoionization and the electronic Kerr effect were developed for coupling with the already established pulse propagation methods.

Distribution Statement

This is block 12 on the SF298 form.

Distribution A - Approved for Public Release

Explanation for Distribution Statement

If this is not approved for public release, please provide a short explanation. E.g., contains proprietary information.

DISTRIBUTION A: Distribution approved for public release.

SF298 Form

Please attach your SF298 form. A blank SF298 can be found here. Please do not password protect or secure the PDF The maximum file size for an SF298 is 50MB.

S98.pdf

Upload the Report Document. File must be a PDF. Please do not password protect or secure the PDF . The maximum file size for the Report Document is 50MB.

final-report.pdf

Upload a Report Document, if any. The maximum file size for the Report Document is 50MB.

Archival Publications (published) during reporting period:

J.R. Gulley, J. Liao, and T.E. Lanier," Plasma generation by ultrashort multi-chromatic pulses during nonlinear propagation," Frontiers in Ultrafast Optics: Biomedical, Scien- tific, and Industrial Application XIV, Proc. SPIE Int. Soc. Opt. Eng. 8972, 89720T (2014).

J. R. Gulley and T. E. Lanier,"Model for ultrashort laser-pulse induced ionization dynamics in transparent solids," Phys. Rev. B. 90, 155119 (2014).

J. Liao and J. R. Gulley, "Time-frequency control of ultrafast plasma generation in dielectrics," J. Opt. Soc. Am. B 31, 2973-2980 (2014).

T. E. Lanier and J. R. Gulley, "Annular space-time focusing in fused silica," Frontiers in Optics 2015, OSA Technical Digest, paper FTu5E.6 (2015).

T. E. Lanier and J. R. Gulley, "Calculation of nonlinear optical damage from space- time-tailored pulses in dielectrics," Laser-Induced Damage in Optical Materials: 2015, Proc. SPIE Int. Soc. Opt. Eng. 9632, 96320Z (2015).

J. R. Gulley and T. E. Lanier, "Self-consistent modeling of photoionization and the Kerr effect in bulk solids," Laser-Induced Damage in Optical Materials: 2015, Proc. SPIE Int. Soc. Opt. Eng. 7632, 96320X (2015).

T. E. Lanier and J. R. Gulley, "Nonlinear space-time focusing and filamentation of annular femtosecond pulses in dielectrics," J. Opt. Soc. Am. B 33, 292-301 (2016).

K. Huthmacher, A. K. Molberg, B. Rethfeld, and J. R. Gulley, "A C++11/Fortran 2003 interface to include electron-electron collisions via Monte Carlo in Multiple Rate Equation simulations," J. Comput. Phys. (under review).

Changes in research objectives (if any):

Change in AFOSR Program Manager, if any:

Extensions granted or milestones slipped, if any:

AFOSR LRIR Number

LRIR Title

Reporting Period

Laboratory Task Manager

Program Officer

Research Objectives

Technical Summary

Funding Summary by Cost Category (by FY, $K)

	Starting FY	FY+1	FY+2
Salary			
Equipment/Facilities			
Supplies			
Total			

Report Document

Report Document - Text Analysis

Report Document - Text Analysis

Appendix Documents

2. Thank You

E-mail user

Apr 30, 2016 09:32:00 Success: Email Sent to: jgulley@kennesaw.edu